PHYSICAL REVIEW E **86**, 040701(R) (2012)

Competition of elasticity and flexoelectricity for bistable alignment of nematic liquid crystals on patterned substrates

T. J. Atherton
Department of Physics and Astronomy, Tufts University, 4 Colby Street, Medford, Massachusetts 02155, USA

J. H. Adler
Department of Mathematics, Tufts University, 503 Boston Avenue, Medford, Massachusetts 02155, USA

(Received 1 August 2012; published 18 October 2012)

We show that patterned surfaces can promote bistable configurations of nematics for reasons other than the symmetry of the surface. Numerical and analytical calculations reveal that a nematic liquid crystal in contact with a striped surface is subject to the competing aligning influences of elastic anisotropy, differing energy cost of various types of deformation, and flexoelectricity, curvature-induced spontaneous polarization. These effects favor opposing ground states where the azimuthal alignment is, respectively, parallel or perpendicular to the stripes. Material parameters for which the effect might be observed lie within the range measured for bent-core nematogens.

DOI: 10.1103/PhysRevE.86.040701 PACS number(s): 61.30.Hn

Complex fluids, such as nematic liquid crystals, exhibit a rich variety of structures when confined to a complicated geometry; for example, a surface prepared with topographic or geometric patterning promotes regions of different molecular orientation. Alignment has been demonstrated with a variety of patterning techniques such as nanoimprinting [1], scribing with the tip of an atomic force microscope [2], lithographic exposure of photoalignable polymer films [3], and microcontact printing [4]. More than one stable configuration may exist, which is essential for applications such as electronic-paper displays [2,3,5,6] and chemical sensing [7,8]. Experimentally demonstrated geometries [1,2,5,9] rely on the symmetry of the surface to provide degenerate states, while in the zenithal bistable device (ZBD) [6], the bistability arises from movable defects induced by a deep grating etched on the surface. In the present Rapid Communication, we identify a different mechanism to achieve bistability in which the stable configurations are each favored by opposing physical effects.

Elastic anisotropy, the dissimilar energy cost of different types of deformation, has been identified as one possible cause of the observed alignment of nematics on patterned surfaces [10,11]. Adjacent to the substrate, the nematic is distorted by the pattern and becomes uniformly aligned away from the surface due to elastic forces. The free energy of the nematic is, famously,

$$F = \frac{1}{2}\int_C K_1(\nabla\cdot\mathbf{n})^2 + K_2(\mathbf{n}\cdot\nabla\times\mathbf{n})^2 + K_3|\mathbf{n}\times\nabla\mathbf{n}|^2 \times d^3x - \frac{1}{2}\int_C \mathbf{D}\cdot\mathbf{E}d^3x - \int_{\partial C} W_\theta(\mathbf{n}\cdot\mathbf{n}_0)^2 d^2x, \quad (1)$$

where the director $\mathbf{n}$ is a headless unit vector field describing the local average orientation of the nematic and where the first three terms represent, in order, splay, twist, and bend deformations with their associated elastic constants. The fourth term represents the interaction of the nematic with the electric field with displacement field $\mathbf{D} = \underline{\epsilon}\cdot\mathbf{E} + \mathbf{P}_{\text{flexo}}$; here, the dielectric tensor is $\underline{\epsilon} = \epsilon_\perp I_3 + \Delta\epsilon\,\mathbf{n}\otimes\mathbf{n}$, where I_3 is the identity matrix, $\epsilon_\parallel$ and $\epsilon_\perp$ are the components parallel and perpendicular to $\mathbf{n}$, respectively, and $\Delta\epsilon = \epsilon_\parallel - \epsilon_\perp$ is the dielectric anisotropy. The final term quantifies the energy cost of $\mathbf{n}$ deviating from the spatially varying preferred orientation, or easy axis, $\mathbf{n}_0$ imposed by the pattern. The coefficient W_θ is referred to as the anchoring energy. The total energy varies as a function of the bulk orientation since different types of deformation are required to comply with the boundary condition imposed by the pattern. One or more effective easy axes may exist that extremize the total elastic energy. On length scales much larger than those of the pattern, the alignment can be described by an effective anchoring potential associated with the surface [12]. A significant advantage of these surfaces over conventional uniform treatments is that the easy axis and anchoring energy can be independently controlled by adjusting the design of the pattern [11–13].

Flexoelectricity, a spontaneous polarization induced by curvature,

$$\mathbf{P}_{\text{flexo}} = e_s\mathbf{n}(\nabla\cdot\mathbf{n}) + e_b\mathbf{n}\times\nabla\times\mathbf{n}, \quad (2)$$

where e_s and e_b are material constants using the sign convention of Rudquist [14], can play a significant role in patterned systems due to the presence of large elastic distortions. It has been identified as important in switching the ZBD [15], in the structure of domain walls [16], as a cause of periodic instabilities [17,18]; it also renormalizes the anchoring in a cell with modulated pretilt [19]. A geometry suggested in the classic work of Meyer [20] to study the flexoelectric effect was a nematic aligned by the electric field of an array of line electrodes held at alternating potential.

In this Rapid Communication, we show that flexoelectricity even in the absence of an external field promotes the alignment of a nematic in contact with a patterned surface and, moreover, that the preferred direction is opposite to that favored by elastic anisotropy. To elucidate the mechanism, we construct a minimal analytical model. Also, careful solution of the full Euler-Lagrange equations using

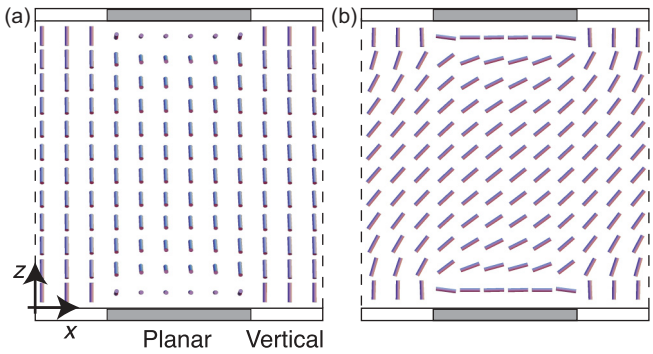

FIG. 1. (Color online) Schematic of system with (a) parallel and (b) perpendicular configuration.

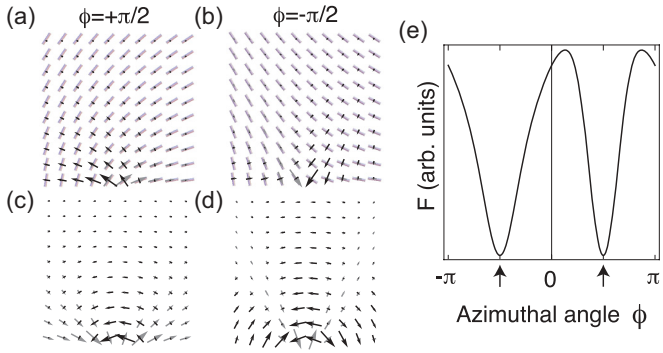

FIG. 2. (Color online) (a) Closeup of the director configuration of a region of nematic adjacent to the boundary between two stripes for $\phi = +\pi/2$. Overlaid arrows indicate the presence of splay-like, $\mathbf{n}(\nabla \cdot \mathbf{n})$, and bendlike, $\mathbf{n} \times \nabla \times \mathbf{n}$, deformations depicted in gray and black, respectively. (b) Corresponding plots for the configuration with $\phi = -\pi/2$. (c) and (d) The associated $\mathbf{D}$ (gray) and $\mathbf{E}$ (black) fields induced by the flexoelectric effect for the configurations shown in (a) and (b). (e) The free energy of this configuration as a function of the azimuthal alignment angle ϕ.

a robust numerical technique allows us to demonstrate that competition between elastic anisotropy and flexoelectricity leads to bistable configurations of the nematic and to identify the range of material parameters over which both states are stable.

The geometry and associated coordinate system under consideration is depicted in Fig. 1 in which a nematic is confined between two symmetric surfaces patterned with stripes that promote, alternatingly, vertical and azimuthally degenerate planar alignment. Two configurations of the nematic that are known to extremize the free energy [11] are depicted, where the bulk orientation is either parallel [Fig. 1(a)] or perpendicular [Fig. 1(b)] to the length of the stripes. The perpendicular configuration consists entirely of splay and bend distortions, while the parallel state contains all three types of distortion present in Eq. (1). For most nematic materials, the twist elastic constant K_2 is lower than the splay K_1 and bend K_3 constants, so the parallel structure represents the ground state as demonstrated in previous experimental [10] and theoretical [11] work.

Flexoelectricity leads to an alignment in this geometry since only splay and bend distortions contribute to the polarization (2) and these distortions are present in different amounts. Consider the region of nematic in the vicinity of the boundary between a vertical and planar stripe, as illustrated in Figs. 2(a) and 2(b): Locally, the director is described by

$$\mathbf{n} = (\cos\theta \sin\phi, \cos\theta \cos\phi, \sin\theta),$$
$$\theta(x,z) = \frac{1}{2}\arctan\left(\frac{x}{z+L_\theta}\right). \tag{3}$$

The configuration (3) minimizes (1) if $K_1 = K_2 = K_3$ for a semi-infinite system where the regions $x < 0$ and $x \geqslant 0$ at $z = 0$ promote vertical and planar alignment, respectively. The anchoring parameter, $L_\theta = K_1/W_\theta$, measures the relative strength of the elastic forces and the surface anchoring; as $L_\theta \to 0$, a sharp transition from planar to vertical orientation is recovered. The electric field induced by this polarization is found by introducing an electrostatic potential $\mathbf{E} = -\nabla V$ and requiring $\nabla \cdot \mathbf{D} = 0$,

$$\epsilon \nabla^2 V = \nabla \cdot \mathbf{P}_{\text{flexo}}. \tag{4}$$

The dielectric anisotropy is temporarily neglected by setting $\epsilon \equiv \epsilon_\perp = \epsilon_\parallel$. The flexoelectric polarization induced in this configuration contains a component with nonzero divergence,

$$\nabla \cdot \mathbf{P}_{\text{flexo}} = (e_s - e_b)\frac{x\{2x^2 + (L_\theta + z)^2(3\cos 2\phi - 7) + 4[x^2 - 2(L_\theta + z)^2]\sin\phi\}}{8[x^2 + (L_\theta + z)^2]^{5/2}}, \tag{5}$$

which, assuming a perfectly matched boundary condition at $z = 0$, yields a potential,

$$V = (e_s - e_b)\frac{x\{3(L_\theta + z)^2 - [2x^2 + 3(L_\theta + z)^2]\cos 2\phi + 4x^2 \sin\phi\}}{24[x^2 + (L_\theta + z)^2]^{3/2}\epsilon}. \tag{6}$$

The associated $\mathbf{D}$ and $\mathbf{E}$ fields are displayed in Figs. 2(c) and 2(d) for $\phi = +\pi/2$ and $\phi = -\pi/2$, respectively. These plots reveal that since $\mathbf{D}$ and $\mathbf{E}$ are mutually perpendicular, the electrostatic energy density is everywhere $\frac{1}{2}\mathbf{D} \cdot \mathbf{E} = 0$ and, hence, the flexoelectric-induced electric field itself has zero energy. Nonetheless, a preferred azimuthal alignment still arises due to the dielectric anisotropy: Suppose an infinitesimal difference in the components of the dielectric tensor $\delta\epsilon$ is introduced, then the leading order correction to the free energy is

$$-\frac{\delta\epsilon}{2}\int_C (\mathbf{n} \cdot \mathbf{E})^2 d^3x. \tag{7}$$

Inserting (3) and (6) into Eq. (7) and performing the integration yields an effective surface potential as a function of ϕ,

$$\widetilde{F}(\phi) = -\delta\epsilon \frac{(e_s - e_b)^2}{\epsilon^2} \frac{(-866 + 909\cos 2\phi - 238\cos 4\phi + 35\cos 6\phi + 240\sin\phi + 200\sin 3\phi - 40\sin 5\phi)}{2^{17}} \times \pi \log\left(1 + \frac{z_0}{L_\theta}\right), \tag{8}$$

where z_0 is a cutoff distance for the integration. While it is clear from the plot in Fig. 2(e) that the perpendicular configuration represents the ground state, the energetic maximum actually occurs at a small angle $\phi \approx \pi/8$ to the parallel configuration. Most unusually for an effective anchoring potential, which typically reflects the symmetry of the pattern, (8) contains terms odd in ϕ because *both* the flexoelectric polarization and the elastic distortion each carry an independent sign as may be seen from the plots in Figs. 2(a) and 2(b).

We have therefore demonstrated, within rather restrictive approximations and in an unbounded geometry, a flexoelectricity-induced azimuthal alignment, which favors the opposite state to that preferred by elastic anisotropy if $\Delta\epsilon > 0$; for negative $\Delta\epsilon$ the flexoelectric effect enhances the elastic anchoring mechanism. Relaxing the assumptions by incorporating unequal elastic constants, allowing for azimuthal variations of $\mathbf{n}$, and including dielectric anisotropy of a realistic magnitude will cause both (3) and (6) to be modified; we now wish to establish what becomes of the flexoelectric-aligning effect, which must now compete with the elastic anisotropy, and to investigate the possibility that in some region of the parameter space the competition is matched such that the alignment is bistable. To do so, it is necessary to solve the full nonlinear Euler-Lagrange equations associated with (1) for both V and $\mathbf{n}$ self-consistently. These are numerically challenging to solve because gradients in $\mathbf{n}$, both those from the physical solution and those associated with error, cause large electric fields through the flexoelectric coupling. We do not use the Q-tensor formalism since the system contains no defects.

To proceed, we use a parallel package [21] that implements the robust first-order system least squares (FOSLS) finite-element method [22,23] with Newton linearizations [24], coupled with nested iteration (NI) [25], algebraic multigrid (AMG) [26], and an efficiency-based adaptive local refinement (ALR) scheme [27,28] to solve the discrete system efficiently. This method has been successfully applied to various complex fluid structure problems, e.g., elasticity [29,30] and magneto-hydrodynamics [27,31].

With this formulation, all terms in the equations are written as first-order derivatives of $\mathbf{n}$, V, $\mathbf{E}$ and auxiliary variable $\underline{U} = \nabla\mathbf{n}$; the solution of the system of equations $\mathcal{L}(\mathbf{u}) = \mathbf{f}$ is posed as the minimization of the L^2 norm of the residual $||\mathcal{L}(\mathbf{u}) - \mathbf{f}||_0$, in which these derivatives appear quadratically [22]. This discretization yields symmetric positive definite discrete linear systems, which can be solved effectively with optimal AMG solvers [32], as well as a sharp and reliable *a posteriori* local error estimator [22]. At each step in the solution algorithm, the estimate allows judgements in the grid refinement process to be made based on the anticipated increase in accuracy at the expense of computational cost. As a result, methods such as NI and ALR are employed to make the process more efficient. The combined method allows the solution process to resolve the approximate solution on an optimal grid with an optimal amount of computational work. This is accomplished when a discrete solution is obtained with total error less than a given tolerance, using a minimal number of degrees of freedom [27] and a solver whose computational cost is linearly proportional to the number of degrees of freedom [22,32]

The Euler-Lagrange equations are written as a relaxation scheme,

$$\frac{\partial\mathbf{n}}{\partial t} - \left(\frac{\partial F}{\partial\mathbf{n}} - \nabla\cdot\frac{\partial F}{\partial\underline{U}}\right) = 0, \tag{9}$$

which is solved together with Maxwell's equations $\nabla\cdot\mathbf{D} = 0$ and $\nabla\times\mathbf{E} = 0$, the definitions $\underline{U} - \nabla\mathbf{n} = 0$ and $\mathbf{E} + \nabla V = 0$, and the auxiliary constraints $\mathbf{n}\cdot\mathbf{n} - 1 = 0$ and $\nabla\times\underline{U} = 0$. These last curl equations are added to ensure that the error estimate is sharp and reliable [22,28]. As this method is derived via a least-squares minimization, consistent equations can be added freely to the system. If done correctly, this allows the norm in which the minimization is done (L^2) to be equivalent to the norm of the error in the solution space (H^1). The addition of these equations guarantees that the error of the solution and all of its derivatives are reduced as expected when the resolution is refined. Since the equations contain many nonlinear terms, NI allows the solver to perform many of the expensive linearizations on coarse grids and only a few at the finest resolutions.

Boundary conditions are imposed as follows: periodic boundaries in the x direction, with $V = 0$ and $\mathbf{n}_0 = (\cos\theta_0\sin\phi_0, \cos\theta_0\cos\phi_0, \sin\theta_0)$ at the top and bottom surfaces. Here,

$$\theta_0(x) = \frac{\pi}{4} + \frac{1}{2}(\arctan\chi_+ - \arctan\chi_-),$$
$$\chi_\pm = \frac{(\xi - 1)\sin(2\pi x)}{(\xi - 1)\cos(2\pi x) \pm 1}. \tag{10}$$

The parameter ξ characterizes the merging of vertical and planar alignment; in the limiting case $\xi \to 0$, a discontinuous transition between stripes occurs, while for $\xi \to \infty$, the surface angle $\theta_0 \to \pi/4$ represents complete mixing. To find the preferred azimuthal anchoring alignment for various physical parameters, a sequence of simulations was performed for which ϕ_0 was set to a constant. Parameters used unchanged between simulations were those for the nematic material 5CB, i.e., $K_1 = 1\times10^{-11}$ N, $\epsilon_\parallel = 18.5$, $\epsilon_\perp = 7$. A value of the anchoring parameter $\xi = 0.05$ was chosen consistent with Ref. [33].

The alignment in the absence of flexoelectricity was first characterized by examining calculated values of F as a function of ϕ_0 such as those shown in Fig. 3(a) for typical values $K_2/K_1 = 1/2$ and $K_3/K_1 \in \{1, 3/2\}$. Regions of the K_2/K_1 and K_3/K_1 parameter space are identified where parallel or perpendicular alignment is favored; these are displayed in Fig. 3(b), together with the critical line along

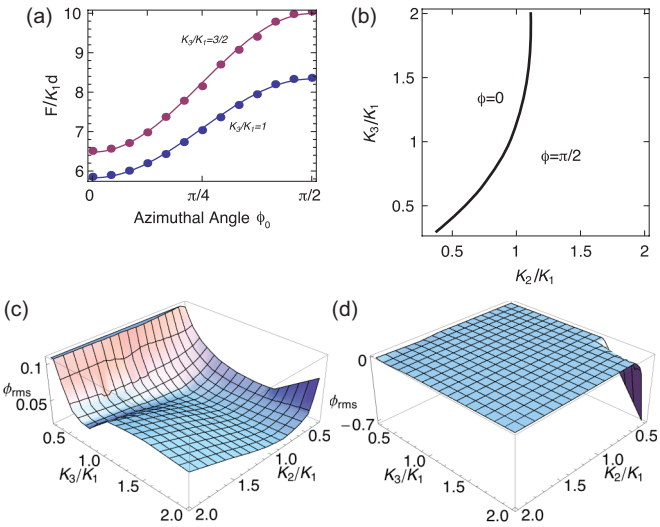

FIG. 3. (Color online) (a) Free energy as a function of ϕ_0 for $K_2/K_1 = 1/2$ with (blue/dark gray) $K_3/K_1 = 1$ and (purple/gray) $K_3/K_1 = 3/2$. (b) Region of K_2/K_1 and K_3/K_1 parameter space where the parallel and perpendicular configurations each represent the ground state. Rms measure of the azimuthal variations of the director for the (c) parallel and (d) perpendicular case.

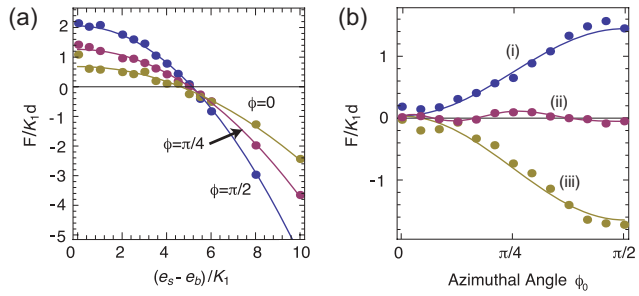

FIG. 4. (Color online) Free energy (a) as a function of $e_s - e_b$ for $\phi_0 \in \{0,\pi/4,\pi/2\}$ and (b) as a function of ϕ_0 for $(e_s - e_b)/K_1 =$ (i) 2, (ii) 5.5, and (iii) 8 C m^{-1}.

which the states become degenerate. In all cases, the extrema of (1) are found to lie at either $\phi = 0$ or $\phi = \pi/2$. The amount of azimuthal variation present in the calculated director profiles, measured by the rms value of ϕ over the domain, is shown in Figs. 3(c) and 3(d). For parallel alignment, out of plane distortions were present where either K_2 or K_3 were much less than K_1. Indeed, the EL equations appear to become unstable if either K_2/K_1 or K_3/K_1 is less than about 0.3. The perpendicular configuration appears more stable with respect to azimuthal variations, which are only observed for small K_2 and large K_3. These results broadly support the approximations used in Refs. [11,33]; they also suggest that, for highly anisotropic elastic constants, configurations where the director varies in two dimensions (2D) become unstable with respect to three-dimensional (3D) variations of the director, for example, a modulation along the length of the stripes. Such instabilities are well known to occur in systems with highly anisotropic elastic constants [34]. This possibility is to be explored in future work, but seems to place a limit on the extent to which behavior at a patterned interface can be controlled by tuning the elastic constants of the nematic material.

A second set of simulations was performed where the combination of flexoelectric parameters $e_s - e_b$ pertinent to the effect as deduced in Eq. (5) was varied. The resulting total free energy is plotted as a function of $e_s - e_b$ in Fig. 4(a), confirming the quadratic dependence predicted in (8) showing that the parallel and perpendicular configurations become degenerate for $(e_s - e_b)/K_1 \sim 5.6$ C J^{-1}. Studying the individual contributions to the free energy, it is found that the numerical noise is greatest on the electric field terms as predicted since the effect of the flexoelectric coupling is to amplify the curvature of the director, which is itself subject to noise. Displaying the total free energy as a function of the azimuthal angle ϕ_0 as in Fig. 4(b) confirms that for $(e_s - e_b)/K_1 = 5.5$ C J^{-1}, the parallel and perpendicular configurations are approximately degenerate and separated by a shallow energy barrier. The calculations agree with the analytical model in that while the perpendicular configuration, $\phi = \pi/2$, is indeed one of the ground states, the other lies at an azimuthal angle of about $\pi/8$ to the parallel state. Examining the behavior of F for three angles $\phi_0 \in \{0,\pi/4,\pi/2\}$ as shown in Fig. 4(a) shows that the region of parameter space over which the bistability occurs is rather limited, confined to $5.5 \lesssim (e_s - e_b)/K_1 \lesssim 5.7$.

The anchoring transition predicted by our model ought to be experimentally observable. Conventional nematic materials are experimentally found to possess quite small flexoelectric coefficients, e.g., for the material E7, Jewell *et al.* [35] obtained $e_s - e_b = +1.5 \times 10^{-11}$ C m^{-1}, while for a proprietary material, Elston measured $|e_s - e_b| = 8 \times 10^{-12}$ C m^{-1} [16]; these results correspond to values of $(e_s - e_b)/K_1 \sim 0.8$–1.5. Even so, the predicted anchoring energies for patterned surfaces should be moderately rescaled by flexoelectricity. Recently, however, bent-core nematogens have been synthesized with flexoelectric coefficients measured to be as high as 3.5×10^{-8} C m^{-1} [36]. It seems likely then that an appropriate mixture or material can be synthesized with parameters suitable for exploiting the alignment and bistable effects.

To study the flexoelectric alignment mechanism in isolation, a number of physical effects have been neglected. First, spatial variation of the ordering, including the possibility of biaxial ordering at the vertical-planar boundary, will adjust the strength of the aligning effect. The presence of mobile ions, as is well known [37], screens the flexoelectric response of the system and, hence, reduces the anchoring. Weak anchoring in earlier work on patterned surfaces [33] simply rescaled the absolute value of the free energy and, hence, ought to affect both states similarly here. A second consequence of using the rigid anchoring approximation is that surfacelike elasticity is neglected, which is known to cause interesting instabilities in other geometries [38]; this is presently being studied together with the apparent instability of the configurations here for very anisotropic elastic constants. Moreover, it remains to study the dynamics of this system to identify the optimal switching strategy; interesting nematodynamical effects such as backflow and kickback are expected in these geometries due to the presence of large gradients. The robust numerical method described is well suited to such problems and will help bring more insight into the problem.

To conclude, we have demonstrated that flexoelectricity causes an azimuthal alignment effect for a nematic in contact with striped substrates due to the coupling of the director to the curvature-induced electric field through dielectric anisotropy, extending the rich physics exhibited by complex fluids in complicated geometries. Moreover, the preferred bulk orientation favored by this effect is opposite to that promoted by elasticity. The competition between the two effects leads to an anchoring transition or bistability within a region of parameter space accessible with recently synthesized bent-core materials.

The authors thank B. Mbanga and C. Burke for helpful discussions, Tufts University for seed funding and for use of the Tufts Linux Research Cluster to perform the calculations presented herein, as well as the computational math group at CU Boulder for their assistance with software packages.

[1] Y. Yi, V. Khire, C. Bowman, J. Maclennan, and N. Clark, J. Appl. Phys. **103**, 093518 (2008).
[2] J. H. Kim, M. Yoneya, and H. Yokoyama, Nature (London) **420**, 159 (2002).
[3] M. Stalder and M. Schadt, Liq. Cryst. **30**, 285 (2003).
[4] J. P. Bramble, S. D. Evans, J. R. Henderson, C. Anquetil, D. J. Cleaver, and N. J. Smith, Liq. Cryst. **34**, 1059 (2007).
[5] S. Kitson and A. Geisow, Appl. Phys. Lett. **80**, 3635 (2002).
[6] G. P. Bryan-Brown, C. V. Brown, J. C. Jones, E. L. Wood, I. C. Sage, P. Brett, and J. Rudin, SID Int. Symp. Dig. Tech. Papers **XXVIII**, 37 (1997).
[7] R. Shah and N. Abbott, Science **293**, 1296 (2001).
[8] M. McCamley, M. Ravnik, A. Artenstein, S. Opal, S. Zumer, and G. Crawford, J. Appl. Phys. **105**, 123504 (2009).
[9] J. H. Kim, J. Yoneya, J. Yamamoto, and H. Yokoyama, Appl. Phys. Lett. **78**, 3055 (2001).
[10] B.-w. Lee and N. A. Clark, Science **291**, 2576 (2001).
[11] T. J. Atherton and J. R. Sambles, Phys. Rev. E **74**, 022701 (2006).
[12] L. Harnau, S. Kondrat, and A. Poniewierski, Phys. Rev. E **76**, 051701 (2007).
[13] G. Barbero, T. Beica, A. L. Alexe-Ionescu, and R. Moldovan, J. Phys. II France **2**, 2011 (1992).
[14] P. Rudquist and S. T. Lagerwall, Liq. Cryst. **23**, 503 (1997).
[15] A. J. Davidson and N. J. Mottram, Phys. Rev. E **65**, 051710 (2002).
[16] S. J. Elston, Phys. Rev. E **78**, 011701 (2008).
[17] M. Monkade, P. Martinot-Lagarde, and G. Durand, Europhys. Lett. **2**, 299 (1986).
[18] G. Barbero and G. Durand, Phys. Rev. A **35**, 1294 (1987).
[19] G. Barbero, G. Skačej, A. L. Alexe-Ionescu, and S. Žumer, Phys. Rev. E **60**, 628 (1999).
[20] R. B. Meyer, Phys. Rev. Lett. **22**, 918 (1969).
[21] M. Brezina, J. Garcia, T. Manteuffel, S. McCormick, J. Ruge, and L. Tang, Numer. Linear Algebra Appl. **19**, 343 (2012).
[22] Z. Cai, R. Lazarov, T. A. Manteuffel, and S. F. McCormick, SIAM J. Numer. Anal. **31**, 1785 (1994).
[23] Z. Cai, T. A. Manteuffel, and S. F. McCormick, SIAM J. Numer. Anal. **34**, 425 (1997).
[24] A. Codd, T. Manteuffel, and S. McCormick, SIAM J. Numer. Anal. **41**, 2197 (2003).
[25] G. Starke, Computing **64**, 323 (2000).
[26] A. Brandt, S. F. McCormick, and J. Ruge, in *Sparsity and Its Applications* (Cambridge University Press, Cambridge, UK, 1984), Chap. 10, pp. 257–284.
[27] J. H. Adler, T. A. Manteuffel, S. F. McCormick, J. W. Nolting, J. W. Ruge, and L. Tang, SIAM J. Sci. Comput. **33**, 1 (2011).
[28] H. DeSterck, T. Manteuffel, S. McCormick, J. Nolting, J. Ruge, and L. Tang, J. Numer. Linear Algebra Appl. **15**, 249 (2008).
[29] Z. Cai, T. A. Manteuffel, S. F. McCormick, and S. V. Parter, SIAM J. Numer. Anal. **35**, 320 (1998).
[30] A. Schwarz, J. Schröder, and G. Starke, Int. J. Numer. Methods Eng. **81**, 286 (2010).
[31] J. H. Adler, T. A. Manteuffel, S. F. McCormick, J. W. Ruge, and G. D. Sanders, SIAM J. Sci. Comput. **32**, 1506 (2010).
[32] X. Zhang, Numer. Math. **63**, 521 (1992).
[33] T. J. Atherton, Liq. Cryst. **37**, 1225 (2010).
[34] F. Lonberg and R. B. Meyer, Phys. Rev. Lett. **55**, 718 (1985).
[35] S. Jewell and J. Sambles, J. Appl. Phys. **92**, 19 (2002).
[36] J. Harden, B. Mbanga, N. Éber, K. Fodor-Csorba, S. Sprunt, J. T. Gleeson, and A. Jákli, Phys. Rev. Lett. **97**, 157802 (2006).
[37] S. Perlmutter, D. Doroski, and G. Moddel, Appl. Phys. Lett. **69**, 1182 (1996).
[38] G. Barbero and V. M. Pergamenshchik, Phys. Rev. E **66**, 051706 (2002).